

Perfect Lattice Topology: The Quantum Rotor as a Test Case ¹

W. Bietenholz^a, R. Brower^b, S. Chandrasekharan^c and U.-J. Wiese^c

^a HLRZ c/o Forschungszentrum, Jülich
52425 Jülich, Germany

^b Department of Physics
Boston University
Boston MA 02215, USA

^c Center for Theoretical Physics
Laboratory for Nuclear Science and Department of Physics
Massachusetts Institute of Technology
Cambridge MA 02139, USA

Preprint MIT-CTP 2583, HLRZ 01/97

Lattice actions and topological charges that are classically and quantum mechanically perfect (i.e. free of lattice artifacts) are constructed analytically for the quantum rotor. It is demonstrated that the Manton action is classically perfect while the Villain action is quantum perfect. The geometric construction for the topological charge is only perfect at the classical level. The quantum perfect lattice topology associates a topological charge distribution, not just a single charge, with each lattice field configuration. For the quantum rotor with the classically perfect action and topological charge, the remaining cut-off effects are exponentially suppressed.

¹This work is supported in part by funds provided by the U.S. Department of Energy (D.O.E.) under cooperative research agreement DE-FC02-94ER40818.

Introduction

The most severe systematic errors in numerical simulations of lattice field theories are due to finite lattice spacing effects. For asymptotically free theories like QCD, Hasenfratz and Niedermayer [1] realized that in the classical limit one can numerically construct nonperturbative perfect lattice actions, which are completely free of finite lattice spacing artifacts. Using the classically perfect action of the 2-d $O(3)$ model even in the quantum theory, they found that cut-off effects are still practically eliminated. A similar behavior has been observed in the 4-d pure $SU(3)$ gauge theory [2], and it has been argued that in these cases the classically perfect action is also quantum perfect at the 1-loop level. This has been demonstrated explicitly for the 2-d $O(3)$ model [3]. In the Gross-Neveu model at large N , the classically perfect action is also perfect at the quantum level for arbitrarily short correlation lengths [4]. The same is true for the $O(N)$ model at large N . Still, one expects that in general a classically perfect action will not be quantum perfect. In this paper we investigate this question in a simple model — the quantum rotor (or 1-d XY model). In this case both, the classically and quantum perfect actions can be constructed analytically. In particular, when the classically perfect action is used at the quantum level, the size of the remaining cut-off effects can be analyzed in detail.

The topological charge of a field configuration on the lattice is usually defined by some smooth interpolation. If one uses the standard lattice formulation, the artifacts are notoriously large. A better definition was proposed by Berg and Lüscher [5] and is referred to as the geometric method. This definition has the virtue that the topological charge is always an integer. However, artifacts can still be significant for rough configurations. Here we use the quantum rotor to formulate a perfect prescription for the topology of lattice configurations. This can be done explicitly since the model is exactly solvable.

The quantum rotor is an ideal test case for perfect lattice topology. One can introduce a topological charge and a θ -vacuum parameter in analogy to QCD. In the 2-d $O(3)$ model the classically perfect topological charge has been constructed in Ref.[6]. Similar constructions have been carried out in the 2-d CP^3 model [7] and in 4-d pure $SU(2)$ gauge theory [8]. Again, the classically perfect topological charge is not perfect at the quantum level. For the quantum rotor the lattice topological charge can be constructed explicitly both at the classical and at the quantum level. This allows us to study the size of the remaining cut-off effects when the classically perfect topological charge is used in the quantum theory. We don't expect the cut-off effects of the quantum rotor to be in quantitative agreement with those of quantum field theory models in higher dimensions. Still, at a qualitative level the analytic study of the quantum rotor tells us how lattice artifacts depend on the correlation length.

The study of the quantum rotor also sheds light on the structure of quantum

perfect lattice topology. It turns out that at the quantum level a lattice field configuration is not just characterized by a single topological charge but by a whole topological charge distribution. This insight may lead to new ways of approximating perfect lattice topology in physically relevant models like QCD.

Transfer Matrix for the Quantum Rotor

We consider a particle of mass M confined to a circle of radius R . This system represents a rotor with moment of inertia $I = MR^2$. The corresponding Hamilton operator reads

$$H = -\frac{\hbar^2}{2I}\partial_\varphi^2, \quad (1)$$

where φ is an angle describing the position of the particle. The energy spectrum of the quantum rotor is given by

$$E_m = \frac{\hbar^2 m^2}{2I}, \quad (2)$$

where $m \in \mathbf{Z}$ specifies the angular momentum. The corresponding wave functions,

$$\langle \varphi | m \rangle = \frac{1}{\sqrt{2\pi}} \exp\{im\varphi\}, \quad (3)$$

are 2π periodic in φ . The above quantum rotor can be modified by changing the Hamilton operator to

$$H(\theta) = -\frac{\hbar^2}{2I} \left(\partial_\varphi - i \frac{\theta}{2\pi} \right)^2. \quad (4)$$

The modified rotor has nontrivial topological properties. The angle θ is analogous to the vacuum angle in QCD. The energy eigenvalues of the modified quantum rotor are

$$E_m(\theta) = \frac{\hbar^2}{2I} \left(m - \frac{\theta}{2\pi} \right)^2, \quad (5)$$

while the wave functions remain unchanged. The partition function for the modified quantum rotor at finite temperature $T = 1/\beta$ is given by

$$Z(\theta) = \text{Tr} \exp\{-\beta H(\theta)\} = \sum_{m \in \mathbf{Z}} \exp\left\{-\frac{\beta \hbar^2}{2I} \left(m - \frac{\theta}{2\pi}\right)^2\right\}. \quad (6)$$

From the partition function one derives the topological charge distribution,

$$p(Q) = \frac{1}{2\pi} \int_{-\pi}^{\pi} d\theta Z(\theta) \exp\{-i\theta Q\} = \sqrt{\frac{2\pi I}{\beta \hbar^2}} \exp\left\{-\frac{2\pi^2 I}{\beta \hbar^2} Q^2\right\}, \quad (7)$$

and from that the topological susceptibility

$$\chi_t = \frac{1}{\beta} \frac{\sum_{Q \in \mathbf{Z}} Q^2 p(Q)}{\sum_{Q \in \mathbf{Z}} p(Q)} = \frac{1}{\beta} \frac{\sum_{Q \in \mathbf{Z}} Q^2 \exp\{-2\pi^2 I Q^2 / \beta \hbar^2\}}{\sum_{Q \in \mathbf{Z}} \exp\{-2\pi^2 I Q^2 / \beta \hbar^2\}}. \quad (8)$$

In the zero temperature limit $\beta \rightarrow \infty$ one obtains

$$\chi_t = \left. \frac{d^2 E_0(\theta)}{d\theta^2} \right|_{\theta=0} = \frac{\hbar^2}{4\pi^2 I}. \quad (9)$$

Using the energy gap at $\theta = 0$, we introduce a correlation time (correlation length in Euclidean time)

$$\xi = \frac{\hbar}{E_1 - E_0} = \frac{2I}{\hbar}, \quad (10)$$

such that at zero temperature

$$\frac{\chi_t \xi}{\hbar} = \frac{1}{2\pi^2}. \quad (11)$$

To formulate the path integral for the quantum rotor on a Euclidean time lattice with lattice spacing a , we first construct the transfer matrix,

$$\begin{aligned} \langle \varphi_{t+a} | \mathcal{T} | \varphi_t \rangle &= \langle \varphi_{t+a} | \exp\left\{-\frac{a}{\hbar} H(\theta)\right\} | \varphi_t \rangle \\ &= \sum_{m \in \mathbf{Z}} \langle \varphi_{t+a} | m \rangle \exp\left\{-\frac{\hbar a}{2I} \left(m - \frac{\theta}{2\pi}\right)^2\right\} \langle m | \varphi_t \rangle \\ &= \frac{1}{2\pi} \sum_{m \in \mathbf{Z}} \exp\left\{-\frac{\hbar a}{2I} \left(m - \frac{\theta}{2\pi}\right)^2 + im(\varphi_{t+a} - \varphi_t)\right\}. \end{aligned} \quad (12)$$

Hence, the Fourier transform of the transfer matrix with respect to $\varphi = \varphi_{t+a} - \varphi_t$ is $\exp\{-\hbar a(m - \theta/2\pi)^2/2I\}/2\pi$. Using the Poisson re-summation formula, the transfer matrix can also be written as,

$$\langle \varphi_{t+a} | \mathcal{T} | \varphi_t \rangle = \sqrt{\frac{I}{2\pi\hbar a}} \sum_{n \in \mathbf{Z}} \exp\left\{-\frac{I}{2\hbar a} (\varphi_{t+a} - \varphi_t + 2\pi n)^2 + i\frac{\theta}{2\pi} (\varphi_{t+a} - \varphi_t + 2\pi n)\right\}. \quad (13)$$

This follows when we consider the Fourier transform of this expression with respect to φ ,

$$\begin{aligned} &\frac{1}{2\pi} \int_{-\pi}^{\pi} d\varphi \sqrt{\frac{I}{2\pi\hbar a}} \sum_{n \in \mathbf{Z}} \exp\left\{-\frac{I}{2\hbar a} (\varphi + 2\pi n)^2 + i\frac{\theta}{2\pi} (\varphi + 2\pi n) - im\varphi\right\} \\ &= \frac{1}{2\pi} \exp\left\{-\frac{\hbar a}{2I} \left(m - \frac{\theta}{2\pi}\right)^2\right\}, \end{aligned} \quad (14)$$

which agrees with the Fourier transform of the expression in Eq.(12).

The exact partition function can be written as a path integral on a Euclidean time lattice with $N = \hbar\beta/a$ points. Starting from

$$Z = \text{Tr} \exp\{-\beta H\} = \text{Tr} \mathcal{T}^N, \quad (15)$$

one inserts complete sets of states $|\varphi_t\rangle$ at each time step (Chapman-Kolmogoroff equation) and one obtains

$$Z = \int \mathcal{D}\varphi \mathcal{D}n \exp\left\{-\frac{1}{\hbar} S[\varphi, n] + i\theta Q[\varphi, n]\right\}. \quad (16)$$

The measure of the path integral is given by

$$\int \mathcal{D}\varphi \mathcal{D}n = \prod_{t=0}^{(N-1)a} \sqrt{\frac{I}{2\pi\hbar a}} \int_{-\pi}^{\pi} d\varphi_t \sum_{n_{t+a/2} \in \mathbf{Z}}, \quad (17)$$

with periodic boundary conditions $\varphi_{Na} = \varphi_0$. The action takes the form

$$S[\varphi, n] = a \sum_{t=0}^{(N-1)a} \frac{I}{2} \left(\frac{\varphi_{t+a} - \varphi_t + 2\pi n_{t+a/2}}{a} \right)^2. \quad (18)$$

This is the Villain action of the XY model, which — by construction — turns out to be a *quantum perfect action*. In the continuum limit $a \rightarrow 0$, it converges to the continuum action

$$S[\varphi] = \int_0^{\hbar\beta} dt \frac{I}{2} \dot{\varphi}(t)^2. \quad (19)$$

Similarly, the perfect topological charge is given by

$$Q[\varphi, n] = \frac{a}{2\pi} \sum_{t=0}^{(N-1)a} \frac{\varphi_{t+a} - \varphi_t + 2\pi n_{t+a/2}}{a}, \quad (20)$$

which — due to periodicity in time — is equivalent to $Q[\varphi, n] = \sum_{t=0}^{(N-1)a} n_{t+a/2}$. In the continuum limit it turns into

$$Q[\varphi] = \frac{1}{2\pi} \int_0^{\hbar\beta} dt \dot{\varphi}(t). \quad (21)$$

It is interesting that the quantum perfect topological charge is given in terms of both, φ and n . This is in contrast to familiar lattice definitions of the topological charge, which work with the angles alone. If one insists to represent also the perfect topological charge in terms of φ alone, one has to perform the sums over n . This, however, does not result in a single topological charge associated with a configuration $[\varphi]$. Instead, even a single configuration is associated with a whole topological charge distribution

$$p[\varphi](Q) = \prod_{t=0}^{(N-1)a} \sum_{n_{t+a/2} \in \mathbf{Z}} \exp\left\{-\frac{1}{\hbar} S[\varphi, n]\right\} \delta_{Q, Q[\varphi, n]}, \quad (22)$$

and the total topological charge distribution is given by

$$p(Q) = \int \mathcal{D}\varphi p[\varphi](Q). \quad (23)$$

This suggests a new way of thinking about lattice topology. Instead of associating a quantum field configuration with a single topological charge, one should associate it with a whole charge distribution. In fact, one may think of a lattice field configuration as representing an ensemble of continuum field configurations that turn into the lattice configuration under a renormalization group transformation. Then

the topology of the continuum theory is perfectly represented by the lattice field, if one associates with it the topological charge distribution of the corresponding ensemble of continuum configurations. This is exactly what happens for the quantum perfect topological charge. As we will see below, one can explicitly construct renormalization group transformations for which the above perfect action lies on the renormalized trajectory.

Before that let us consider the classical limit $\hbar \rightarrow 0$. Then the path integral turns into a saddle point problem. In particular, for a given configuration φ the variables n adjust themselves such that $(\varphi_{t+a} - \varphi_t + 2\pi n_{t+a/2})^2$ is minimized, i.e. such that $\varphi_{t+a} - \varphi_t + 2\pi n_{t+a/2} = (\varphi_{t+a} - \varphi_t) \bmod 2\pi \in]-\pi, \pi]$. Hence, in the classical limit the perfect action turns into

$$S_c[\varphi] = \sum_{t=0}^{(N-1)a} \frac{I}{2a} ((\varphi_{t+a} - \varphi_t) \bmod 2\pi)^2. \quad (24)$$

This is the so-called Manton action [9], which turns out to be classically perfect. Similarly, the classically perfect topological charge is

$$Q_c[\varphi] = \frac{1}{2\pi} \sum_{t=0}^{(N-1)a} (\varphi_{t+a} - \varphi_t) \bmod 2\pi. \quad (25)$$

This is identical with the geometric topological charge. It is classically but not quantum perfect. The geometric charge is based on a particular interpolation of the lattice variables φ_t along a shortest arc. The quantum perfect charge, on the other hand, emerges when one integrates over all possible interpolations (all paths connecting neighboring lattice variables) with the appropriate Boltzmann weight.

Comparison between Classical and Quantum Perfection

The question arises, how well the classically perfect action and topological charge work at the quantum level. This is an important issue, because in the more complicated models in higher dimensions, we only have the classically perfect quantities at hand. To investigate this question we construct the transfer matrix for the classically perfect action

$$\begin{aligned} \langle \varphi_{t+a} | \mathcal{T}_c | \varphi_t \rangle &= \sqrt{\frac{I}{2\pi\hbar a}} \exp\left\{-\frac{I}{2\hbar a} ((\varphi_{t+a} - \varphi_t) \bmod 2\pi)^2\right\} \\ &\times \exp\left\{i\frac{\theta}{2\pi} (\varphi_{t+a} - \varphi_t) \bmod 2\pi\right\}. \end{aligned} \quad (26)$$

It is straightforward to diagonalize the transfer matrix by performing a Fourier transform. The resulting energy spectrum is given by

$$\exp\left\{-\frac{a}{\hbar} E_m^c(\theta)\right\} = \sqrt{\frac{I}{2\pi\hbar a}} \int_{-\pi}^{\pi} d\varphi \exp\left\{-\frac{I}{2\hbar a} \varphi^2 - i\left(m - \frac{\theta}{2\pi}\right)\varphi\right\}. \quad (27)$$

For the topological susceptibility at zero temperature this implies

$$\chi_t^c = \frac{d^2 E_0^c(\theta)}{d\theta^2} \Big|_{\theta=0} = \frac{\hbar}{4\pi^2 a} \frac{\int_{-\pi}^{\pi} d\varphi \varphi^2 \exp\{-I\varphi^2/2\hbar a\}}{\int_{-\pi}^{\pi} d\varphi \exp\{-I\varphi^2/2\hbar a\}}. \quad (28)$$

Of course, in the continuum limit $a \rightarrow 0$ one reproduces the result of Eq.(9). At large ξ/a , the lattice artifacts are exponentially suppressed as

$$\frac{\chi_t^c \xi}{\hbar} \sim \frac{1}{2\pi^2} - \sqrt{\frac{\pi\xi}{a}} \exp\left\{-\frac{\pi^2\xi}{4a}\right\}. \quad (29)$$

For comparison we also consider the standard action

$$S_s[\varphi] = \sum_{t=0}^{(N-1)a} \frac{I}{a} (1 - \cos(\varphi_{t+a} - \varphi_t)). \quad (30)$$

Using it together with the geometric topological charge one finds

$$\begin{aligned} \langle \varphi_{t+a} | \mathcal{T}_s | \varphi_t \rangle &= \sqrt{\frac{I}{2\pi\hbar a}} \exp\left\{-\frac{I}{\hbar a} (1 - \cos(\varphi_{t+a} - \varphi_t))\right\} \\ &\times \exp\left\{i\frac{\theta}{2\pi} (\varphi_{t+a} - \varphi_t) \bmod 2\pi\right\}. \end{aligned} \quad (31)$$

Again we diagonalize the transfer matrix by performing a Fourier transformation and we arrive at

$$\exp\left\{-\frac{a}{\hbar} E_m^s(\theta)\right\} = \sqrt{\frac{I}{2\pi\hbar a}} \int_{-\pi}^{\pi} d\varphi \exp\left\{-\frac{I}{\hbar a} (1 - \cos\varphi) - i\left(m - \frac{\theta}{2\pi}\right)\varphi\right\}. \quad (32)$$

Now the topological susceptibility at zero temperature takes the form

$$\chi_t^s = \frac{\hbar}{4\pi^2 a} \frac{\int_{-\pi}^{\pi} d\varphi \varphi^2 \exp\{-I(1 - \cos\varphi)/\hbar a\}}{\int_{-\pi}^{\pi} d\varphi \exp\{-I(1 - \cos\varphi)/\hbar a\}}, \quad (33)$$

$$\frac{\chi_t^s \xi}{\hbar} = \frac{1}{2\pi^2} \left(1 + \frac{a}{\xi}\right) + O((a/\xi)^2). \quad (34)$$

Let us compare the magnitude of the cut-off effects for the various actions. Fig.1 shows the ratio of the first two energy gaps $(E_2 - E_0)/(E_1 - E_0)$ at $\theta = 0$ as a function of the correlation time in lattice units, ξ/a . In the continuum limit all actions give the correct answer. At finite a , however, both the standard and the classically perfect action suffer from cut-off effects. The asymptotic suppression of the artifacts at large ξ/a is again power-like respectively exponential,

$$\frac{E_2^s - E_0^s}{E_1^s - E_0^s} = 4\left(1 - \frac{a^2}{\xi^2}\right) + O((a/\xi)^3), \quad (35)$$

$$\frac{E_2^c - E_0^c}{E_1^c - E_0^c} = 4\left(1 + \frac{2}{\pi} \sqrt{\frac{\xi}{a}} \exp\left\{-\frac{\pi^2\xi}{4a} + \frac{a}{\xi}\right\} + \dots\right). \quad (36)$$

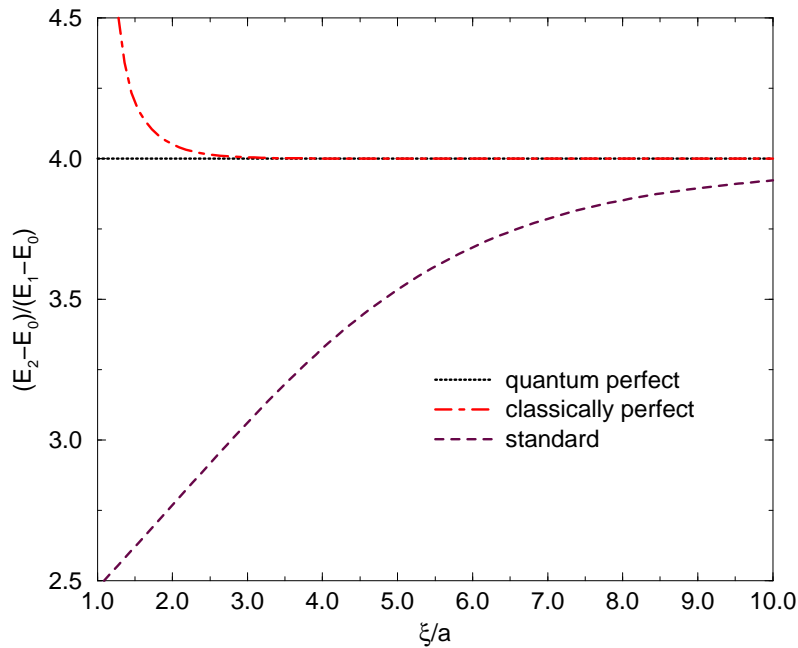


Figure 1: *The ratio of the first two energy gaps $(E_2 - E_0)/(E_1 - E_0)$ as a function of the correlation time in lattice units for the classically and quantum perfect actions and for the standard action.*

At a given ratio ξ/a , the artifacts are much smaller for the classically perfect formulation than for the standard formulation. For example, at $\xi = 2a$ the cut-off effect of the energy ratio is 30.8 percent for the standard action and only 1.3 percent for the classically perfect action. Fig.2 depicts the cut-off effect of $\chi_t \xi/\hbar$ at zero temperature as a function of ξ/a . Again, at $\xi = 2a$ the cut-off effect for the standard action and geometric charge is huge, 60.4 percent to be precise, compared to 1.8 percent for the classically perfect action and topological charge. In this case the artifacts in the standard action are even larger than in the case of the gap ratio, because their suppression is only linear, as we see from Eq.(34).

Quantum Perfect Action and the Renormalization Group

Here we briefly present a more general real space renormalization group derivation of the quantum perfect action for the quantum rotor. This alternative derivation is interesting because it does not rely explicitly on the peculiar simplifications inherent in a 1-d theory and the resulting nearest neighbor form for the perfect action. Above we have made use of the Hamilton operator (or transfer matrix), which is especially simple for a 1-d system since its dynamics is equivalent to ordinary quantum mechanics. In the 1-d case, by integrating the fields on the line segments between each pair of lattice points, one necessarily arrives at a nearest neighbor (or

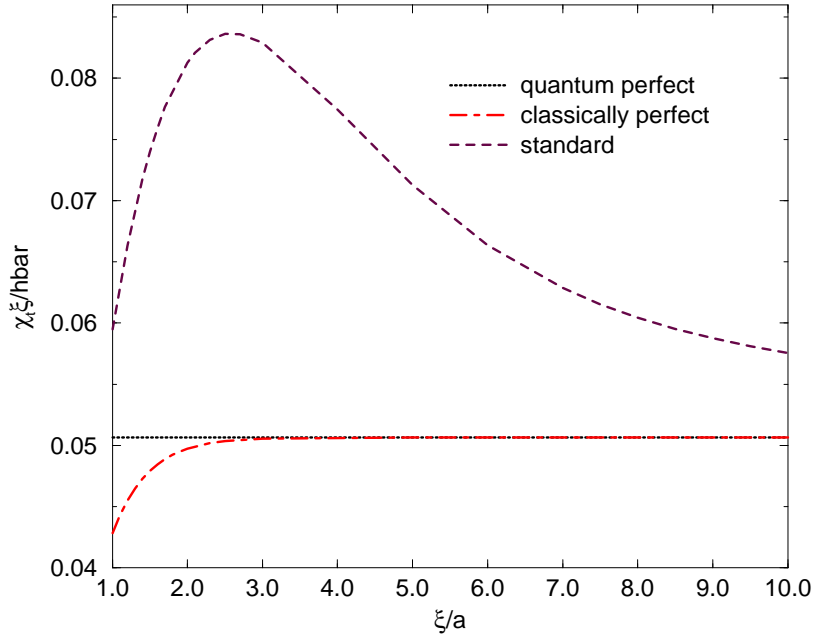


Figure 2: *The product $\chi_t \xi/\hbar$ as a function of the correlation time ξ/a in lattice units for the classically and quantum perfect actions and for the standard action.*

ultra-local) action. Viewed as a renormalization group transformation (RGT), such a procedure is often referred to as “decimation”. However, in higher dimensions decimation is not a satisfactory blocking procedure since it leads to long range interactions that are not exponentially suppressed. Consequently, it is important to ask if our results for the quantum rotor and the qualitative lessons drawn from them are tied to the use of the transfer matrix and ultra-locality.

A more general derivation can be made using a real space RGT for the action in the path integral formalism. In this form, the resulting lattice action need not be ultra-local to formulate the quantum perfect charge. Moreover such RGTs have recently been used successfully to define classically perfect actions in higher dimensions for certain quantum field theories [10, 11] and consequently they could in principle be used to investigate quantum perfect topological features along the lines of this paper. We are aware of the difficulty in carrying out such a task in practice, but it is still important that the quantum rotor example can also be understood in this more general framework.

Let us sketch the derivation of this result. We divide the interval $[0, \hbar\beta]$ into N parts, each with length a , so that $\hbar\beta = aN$. The blocked lattice field, ϕ , is related to the continuum field, φ , by averaging over a cell of length a centered at the lattice

site t . Thus

$$\phi_t = \frac{1}{a} \int_{t-a/2}^{t+a/2} dt' \varphi(t') \equiv \int dt' \Pi(t' - t) \varphi(t') , \quad (37)$$

where the Haar function is $\Pi(t) = 1/a$ inside the cell $t \in [-a/2, a/2]$ and zero outside. In contrast, the transfer matrix approach uses the value at the lattice site, which corresponds to setting $\Pi(t' - t) = \delta(t' - t)$ in Eq.(37). In fact, there is one *crucial* detail that has been ignored in the definition of the blocking prescription. Since the action is really a function of the compact fields, $u(t) = \exp\{i\varphi(t)\}$, this blocking procedure must be applied mod 2π . To define the perfect action, it will also be convenient to generalize the blocking procedure with Gaussian smearing.

Thus an exact perfect action can be defined by

$$\exp\{-\frac{1}{\hbar}S[\phi]\} = \int \mathcal{D}\varphi \exp\{-\frac{1}{\hbar} \int_0^{\hbar\beta} dt' \frac{I}{2} \dot{\varphi}^2(t') + \frac{i\theta}{2\pi} \int_0^{\hbar\beta} dt' \dot{\varphi}(t') - \frac{1}{\hbar} T[\phi, \varphi]\} , \quad (38)$$

where the transformation term,

$$\exp\{-\frac{1}{\hbar}T[\phi, \varphi]\} = \prod_t \sum_{m_t \in \mathbf{Z}} \exp\{-\frac{\hbar a \alpha}{I} m_t m_t + im_t[\phi_t - \int dt' \Pi(t' - t) \varphi(t')]\} , \quad (39)$$

is given by an integer Gaussian transform. The integer sums over m_t guarantee periodicity for the lattice fields, while the hard constraint (37) is re-instated mod 2π in the limit $\alpha \rightarrow 0$, as a special case.

By a straightforward series of steps, the exact integration for this RGT from the continuum to the lattice is performed. The formal steps are similar to those used for the transfer matrix. To perform the integral (38), we first expand in Fourier modes,

$$\varphi(t) = \frac{2\pi Q}{\hbar\beta} t + \sum_k \exp\{\frac{i}{\hbar} E_k t\} \varphi_k , \quad (40)$$

where $E_k = 2\pi\hbar k/(aN)$ and $k \in \mathbf{Z}$. The linear term is present due to non-trivial topological sectors. Then using the Poisson re-summation formula to do the sum over m_t , we are lead to a closed expression for the perfect quantum partition function,

$$Z(\theta) = \int \mathcal{D}\phi \mathcal{D}n \exp\{-\frac{1}{\hbar}S[\phi, n] + i\theta Q[\phi, n]\} . \quad (41)$$

The quantum perfect topological charge density is *exactly* the same as that derived from the transfer matrix, and is given in Eq.(20). However, the quantum perfect action

$$S[\phi, n] = -\frac{I}{2a} \sum_{t=0}^{(N-1)a} \sum_{j=1}^{\infty} \Delta^{-1}(ja) (\phi_{t+ja} - \phi_t + 2\pi(n_{t+a/2+(j-1)a} + \dots + n_{t+a/2}))^2 , \quad (42)$$

generalizes Eq.(18) to allow for non-local couplings through $\Delta^{-1}(ja)$, which fall off exponentially in $|ja|$. Further, ϕ_t and $n_{t+a/2}$ are periodic in t by definition. Thus

for example $n_{t+a/2+(j-1)a} + \dots + n_{t+a/2}$ represents a “gauge” string originating at $t + a/2$ and ending at $t + a/2 + (j - 1)a$, wrapped around the lattice many times as j becomes large. The infinite lattice propagator $\Delta(t)$ in E space,

$$\tilde{\Delta}(E) = \sum_{l \in \mathbf{Z}} \frac{\Pi(E + 2\pi l \hbar/a)^2}{(aE/\hbar + 2\pi l)^2} + \alpha = \frac{1}{\hat{E}^2} - \frac{1}{6} + \alpha, \quad (43)$$

is given by the standard expression for a perfect lattice scalar field (see Ref. [12]) where $\Pi(E) = \hat{E}/E$, with $\hat{E} = (2\hbar/a) \sin(aE/2\hbar)$ being the E space Haar function.

By inspection we see that for $\alpha = 1/6$, $\Delta(t)$ is the standard nearest neighbor lattice propagator and thus the action defined in Eq.(42) becomes ultra-local. Further, this is exactly the quantum perfect action, given in Eq.(18), derived earlier by the transfer matrix method. Consequently, the notion of a quantum perfect charge is unchanged in the standard RGT approach, even with an infinite number of couplings in the perfect action.

Conclusions

We have presented the concept of a quantum perfect topological charge on the lattice, and we have worked it out explicitly for the simple case of a quantum rotor. We found the perfect action to be of the Villain type. This formulation is valid and exact for arbitrarily rough configurations.

Actions of the Villain type occur generally if one maps non-compact continuum fields onto compact lattice variables. They are applicable for the projection of non-compact continuum gauge fields to compact lattice link variables [13]. We also discussed the artifacts in the classically perfect formulation, where the charge coincides with the geometric charge, while the classically perfect action turns out to be the Manton action. These identifications are specific to the simple, exactly solvable model considered here. The artifacts in the classically perfect formulation are exponentially suppressed. They are much smaller than the artifacts in the standard formulation, which disappear only power-like close to the continuum limit.

References

- [1] P. Hasenfratz and F. Niedermayer, Nucl. Phys. B414 (1994) 785.
- [2] T. DeGrand, A. Hasenfratz, P. Hasenfratz and F. Niedermayer, Nucl. Phys. B454 (1995) 587; Nucl. Phys. B454 (1995) 615; Phys. Lett. B365 (1996) 233.
- [3] A. Farchioni, P. Hasenfratz, F. Niedermayer and A. Papa, Nucl. Phys. B454 (1995) 638.
- [4] W. Bietenholz, E. Focht and U.-J. Wiese, Nucl. Phys. B436 (1995) 385.
- [5] B. Berg and M. Lüscher, Nucl. Phys. B190 [FS3] (1981) 412.
M. Lüscher, Comm. Math. Phys. 85 (1982) 39.
- [6] M. Blatter, R. Burkhalter, P. Hasenfratz and F. Niedermayer, Phys. Rev. D53 (1996) 923.
M. D'Elia, F. Farchioni and A. Papa, Phys. Rev. D55 (1997) 2274.
- [7] R. Burkhalter, Phys. Rev. D54 (1996) 4121.
- [8] T. DeGrand, A. Hasenfratz and D. Zhu, Nucl. Phys. B475 (1996) 321;
Nucl.Phys. B478 (1996) 349.
- [9] N. Manton, Phys. Lett. B96 (1980) 328.
- [10] W. Bietenholz and U.-J. Wiese, Phys. Lett. B378 (1996) 222.
- [11] W. Bietenholz and U.-J. Wiese, Nucl. Phys. B464 (1996) 319.
- [12] T. Bell and K. Wilson, Phys. Rev. B11 (1975) 3431.
- [13] W. Bietenholz, R. Brower, S. Chandrasekharan and U.-J. Wiese, in preparation.